ChemPubSoc Europe

DOI: 10.1002/chem.201804826

CHEMISTRY A European Journal Full Paper

Biochemistry

Exploring Rigid and Flexible Core Trivalent Sialosides for Influenza Virus Inhibition

Pallavi Kiran[+],[a] Sumati Bhatia[+],[a] Daniel Lauster,[b] Stevan Aleksić,[c] Carsten Fleck,[d] Natalija Peric,[d] Wolfgang Maison,[d] Susanne Liese,[e, f] Bettina G. Keller,[c] Andreas Herrmann,[b] and Rainer Haag*[a]

Abstract: Herein, the chemical synthesis and binding analysis of functionalizable rigid and flexible core trivalent sialosides bearing oligoethylene glycol (OEG) spacers interacting with spike proteins of influenza A virus (IAV) X31 is described. Although the flexible Tris-based trivalent sialosides achieved micromolar binding constants, a trivalent binder based on a rigid adamantane core dominated flexible tripodal compounds with micromolar binding and hemagglutination inhibition constants. Simulation studies indicated increased conformational penalties for long OEG spacers. Using a systematic approach with molecular modeling and simulations as well as biophysical analysis, these findings emphasize on the importance of the scaffold rigidity and the challenges associated with the spacer length optimization.

Introduction

Annually, seasonal influenza infections pose a great burden to global health and the economy affecting up to 15% of the world population resulting in more than 500 000 deaths per year worldwide.[1] High mutation rates of this virus limit the use of available antiviral agents for a long-lasting application. Thus, there is urgent need for the development of novel antiviral drugs and therapies. A well-known strategy is the application of biomimetic binding inhibitors, acting as decoy molecules to prevent viral attachment to host cells. The latter is mediated by multivalent interaction of the homotrimeric hemagglutinin (HA) spike protein that is highly abundant on the viral surface with terminal sialic acids of glycostructures on the host cell plasma membrane.[2] Each monomer of the HA trimer has a receptor binding site (RBS) for sialic acid (SA). Inhibitors displaying SA moieties and thus competing with virus receptors on host cells, have been successfully implemented in various studies.[2b] Recently, Bandlow et al. reported on micromolar binding constants with bivalent sialyllactose derivatives based on DNA-PNA complexes.[3] Further, Bhatia et al. reported on nanomolar inhibitors of influenza virus infection with linear and dendritic polyglycerol based multivalent sialosides.[4] However, only few examples demonstrated the design of a trivalent binder, which is based on a rational design to match the geometric and topological situation on HA.[3,5]

As revealed from the crystal structure of HA from a human pathogenic H3N2 strain (PDB ID: 1hgg), the planar distance between two SA-binding sites on a single HA trimer is around 4–5 nm (Figure 1).[6] HA trimers are densely packed in the viral envelope and two adjacent HA_3 are 10–12 nm centrally apart as determined from electron microscopy imaging.[7] Considering this spatial HA organization, a high affinity trivalent SA binder can be hypothetically designed by choosing an appropriate spacer to bring three covalently connected SA units in the right geometry matching that of the RBSs of HA_3. Waldmann et al. explored trivalent SA presenting glycopeptide conjugates for targeting HA trimers of influenza A virus type H5 and obtained a binding constant of 446 nM from surface plasmon resonance (SPR) measurements, which is a 4000-fold increase compared to the monomeric binder methyl 2-methyl-α-

[a] P. Kiran,[+] Dr. S. Bhatia,[+] Prof. Dr. R. Haag
Institut für Chemie und Biochemie Organische Chemie
Freie Universität Berlin, Takustr. 3, 14195 Berlin (Germany)
E-mail: haag@zedat.fu-berlin.de

[b] Dr. D. Lauster, Prof. Dr. A. Herrmann
Institut für Biologie, Molekulare Biophysik, IRI Life Sciences
Humboldt-Universität zu Berlin, Invalidenstr. 42, 10115 Berlin (Germany)

[c] Dr. S. Aleksić, Prof. Dr. B. G. Keller
Institut für Chemie und Biochemie, Physikalische und Theoretische Chemie
Freie Universität Berlin, Takustr. 3, 14195 Berlin (Germany)

[d] Dr. C. Fleck, N. Peric, Prof. Dr. W. Maison
Fachbereich Chemie, Institut für Pharmazie
Universität Hamburg, Bundesstr. 45, 20146 Hamburg (Germany)

[e] Dr. S. Liese
Department of Mathematics, University of Oslo
P.O Box 1053 Blinder, 0316 Oslo (Norway)

[f] Dr. S. Liese
Department of Physics, Freie Universität Berlin
Arnimallee 14, 14195 Berlin, (Germany)

[+] These authors contributed equally to this work.

Supporting information and the ORCID identification number(s) for the author(s) of this article can be found under: https://doi.org/10.1002/chem.201804826.

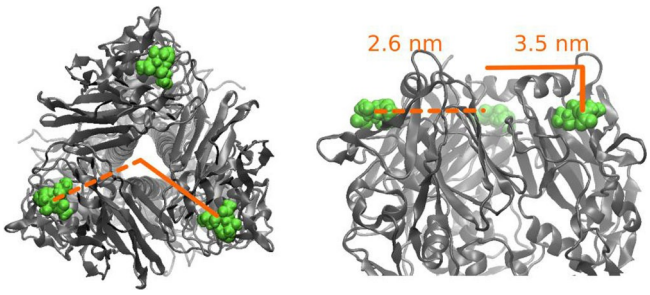

Figure 1. Top view (left) and side view (right) of the HA -region (PDB ID: 1hgg). Bound sialic acid is highlighted in green.

D-*N*-acetylneuraminide (Neu5Acα2Me) or methyl sialic acid, respectively. However, the inhibition values were still weak and in the micromolar range in saturation-transfer difference (STD) NMR based competition experiments. Nishimura and colleagues devised a glycopeptide possessing a cyclic peptides as scaffold [Neu5Acα(2,3)Galβ(1,4)Glc] to display three sialotrisaccharide units at the termini.[8] In further studies, Nishimura et al. prepared trivalent sialyllactosides using trisphenol and trisaniline as cores and extended the length of the spacer with ethylenglycol trimers (EG_3), glutamine, and C_6 to partially compensate for the smaller scaffold.[9] These studies indicated that the design of trivalent binders is still challenging and that there are still several unknown parameters to finetune a trivalent binder for an optimal interaction with HA.

In this study, we address the relevance of the flexibility of the anchor point carrying the sialoside residues for optimal interaction with HA. Furthermore, we varied the spacer length on both a rigid and a flexible core system to adjust the receptor spacing to match the given RBS distribution on HA trimers. The OEG spacers have been used due to their hydrophilicity and biocompatibility. However, the drawback of long OEG spacers is their high tendency to form globular structures, hampering an orchestral receptor orientation. OEG spacer containing HA-binders were implemented first by Knowles et al. for the synthesis of bivalent sialosides that showed 100-fold increased hemagglutination inhibition against influenza A virus X31 (H3N2) as compared to monovalent sialic acid.[10]

In the present study, we systematically explored trivalent sialosides with different OEG lengths using two differently functionalizable core structure with either (i) an adamantane core, and (ii) a commercially available Tris that is, 4-(((benzyloxy)carbonyl)amino)-4-(2-carboxyethly)heptanedioic acid core. Due to a restricted degree of rotational freedom of the anchorage points on the different scaffolds, adamantane can be considered to be more rigid compared to Tris. Here we present the synthesis and comparative analysis of rigid and flexible core based trivalent sialosides with different spacer lengths for binding to IAV-X31 (subtype Aichi) using microscale thermophoresis (MST) and hemagglutination inhibition (HAI) assays. Despite the challenges associated with the spacer length optimization, we could identify an inhibitor against X31 with a HAI value in the micromolar range, thus being approximately 3000-fold more potent compared to monomeric SA. The present study reveals insights into the scaffold selection and spacer length optimization and emphasizes their relevance for the design of trivalent HA binders.

Results and Discussion

Based on the crystal structure of a single HA trimer (PDB ID: 1hgg), we determined the projected distance between the receptor binding sites, and the trimer midpoint of 2.6 nm. The binding site is found about 0.9 nm below the top of the HA surface, which leads to an effective distance of 3.5 nm between the receptor binding sites and the HA midpoint. The part of the tripod has a length of approximately 1.2 nm. Hence the OEG- spacer has to bridge a distance of approximately 2 nm. The length distribution of flexible OEG chains that we obtained from our previous MD simulations,[11] suggested that the OEG-linker must consist of at least 6–14 ethylene glycol units to span the distance between the ligand core and the binding sites (c.f. Supporting Information)

Synthesis of adamantane-based trivalent and bivalent sialosides

Heterobifunctional oligoethylene glycols,[12] tris(2-carboxymethyl)aminoadamantane amine,[13] bis(2-carboxymethyl)aminoadamantaneamine and cbz-protected adamantane triacid,[14] and diacid[15] were prepared as reported in literature. SA-conjugated trivalent derivative with only an ethylene spacer **4** was prepared by using amide coupling with an ethanolamine sialic acid derivative **3** (Scheme 1). While reactions of adamantane triacid were less efficient when done by direct amide coupling of bigger length EG_{14} spacer. Therefore, coupling of cbz-protected adamantane triacid **1** with propargylamine provided an easy way to couple heterobifunctional oligoethylene glycols by a click chemistry approach. The addition of extra triazole units by amide bonds provided the limited flexibility and decreased the length requirements of a flexible OEG spacer. Heterobifunctional azido-tosylated EG_6 and EG_{14} were synthesized as short and long OEG spacers to achieve the predicted OEG requirements. The prop-2-ynyl α-thiosialoside was synthesized

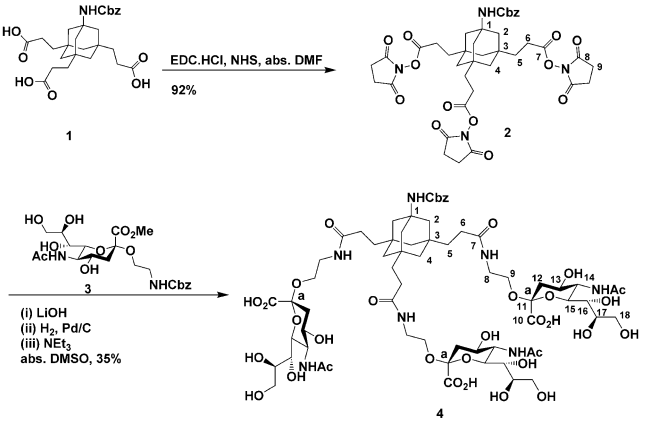

Scheme 1. Synthesis of adamantane core trivalent sialoside with an EG_1 spacer.

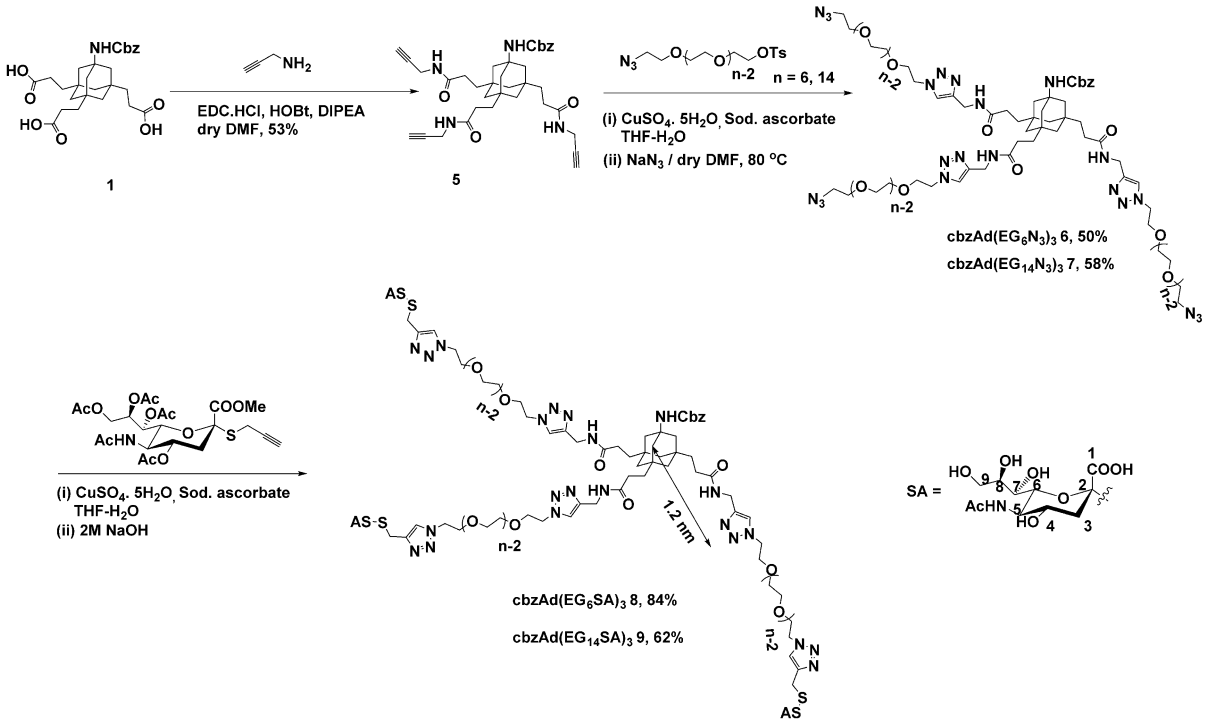

Scheme 2. Synthesis of adamantane core trivalent sialosides with EG_6 and EG_{14} spacers.

using procedure reported by Roy et al.[16] and a slightly modified procedure of Ogura et al.[17] The prop-2-ynyl α-thiosialoside was conjugated by click chemistry to trivalent adamantane derivatives **6** and **7** (Scheme 2). For the preparation of a divalent adamantane sialoside, a heterobifunctional EG_6 spacer bearing azide and sialic acid residues **13** was synthesized and coupled to divalent propargylated adamantane **12**. The adamantane divalent sialoside was prepared to study the depend-

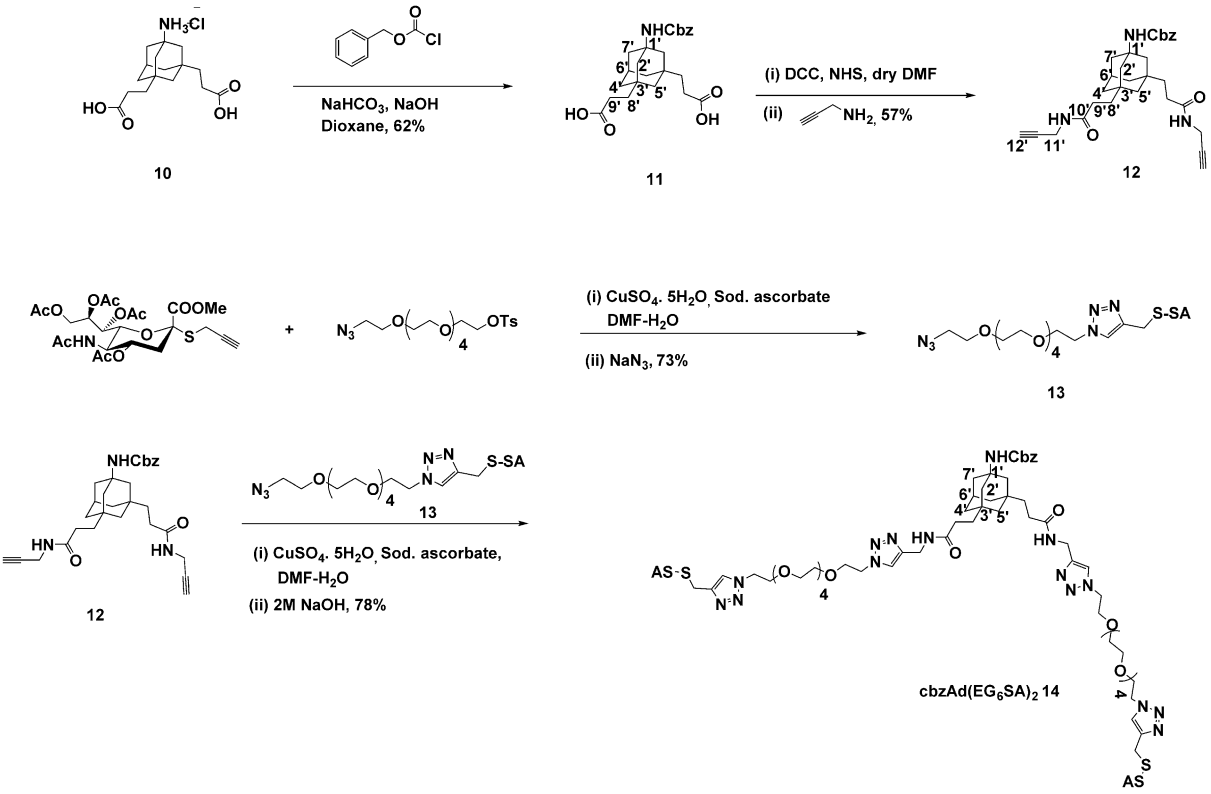

Scheme 3. Synthesis of adamantane core divalent sialoside with EG_6 spacer.

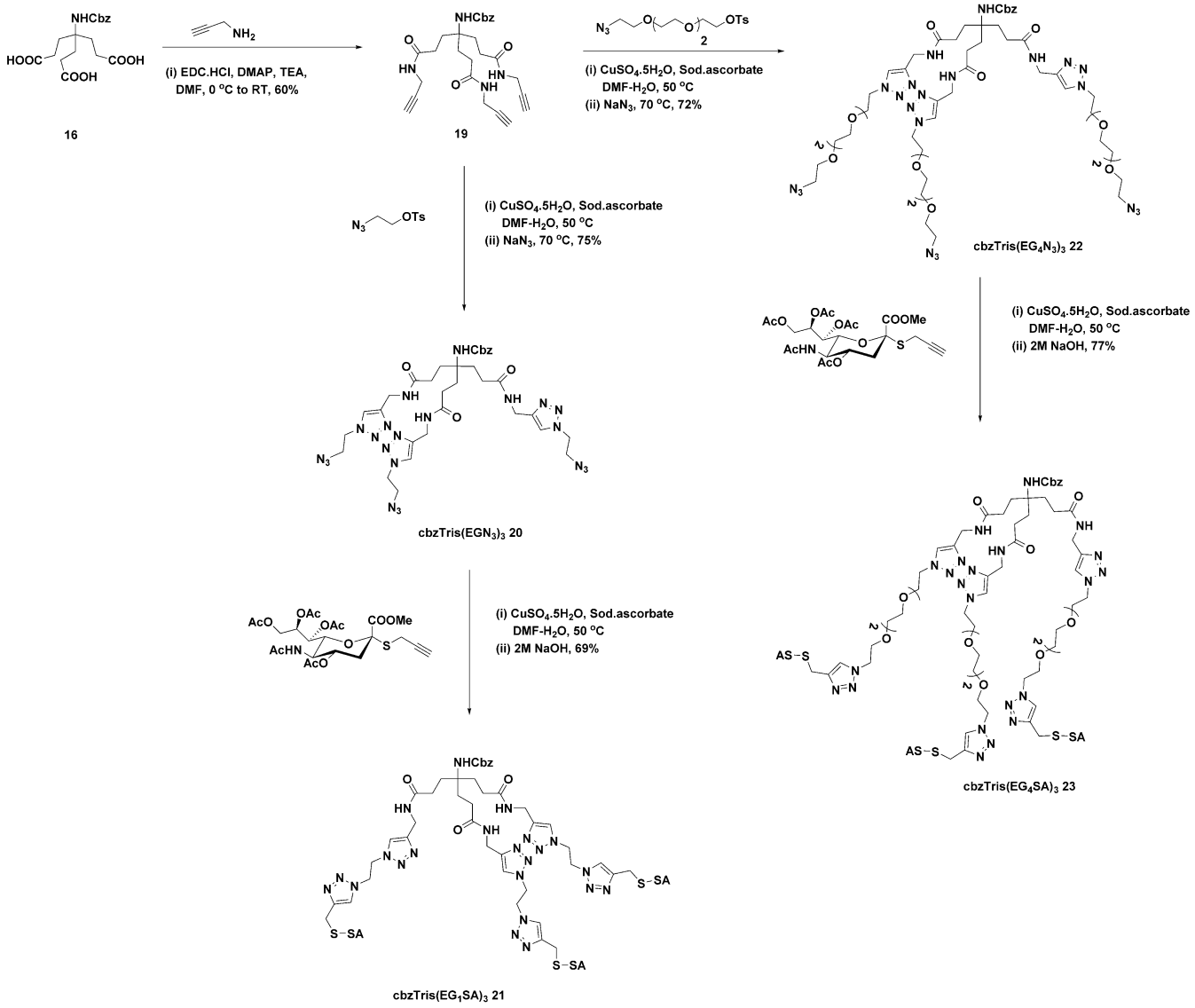

Scheme 4. Synthesis of Tris core trivalent sialoside with EG_7 spacer.

ency of affinity on the presence of 2 versus 3 sialic acid valencies on the rigid core (Scheme 3).

Synthesis of Tris-based trivalent sialosides

4-(((Benzyloxy)carbonyl)amino)-4-(2-carboxyethly)heptanedioic acid **16** was prepared according to literature procedures from di-*tert*-butyl 4-amino-4-(3-(*tert*-butoxy)-3-oxopropyl)heptanedioate **15**[17] followed by coupling with propargylamine to produce tripropagylated derivative **19**. The triazido derivatives cbzTris(EG_4N_3)$_3$ **22** and cbzTris(EGN_3)$_3$ **20** were prepared in two consecutive steps by conjugating heterobifunctional azidotosyl EG_4 and EG_1 units followed by in situ azidation (Scheme 4). Prop-2-ynyl α-thiosialoside was then clicked in a similar fashion as done before to afford the final trivalent sialosides with a flexible core **21** and **23**. Heterobifunctional aminoazido EG_7 was easily obtained from Polypure which was then coupled with 4-(((benzyloxy)carbonyl)amino)-4-(2-carboxyethly)heptanedioic acid **16** using amide coupling (Scheme 5). Prop-2-ynyl α-thiosialoside was clicked with cbzTris(EG_7N_3)$_3$ **17** as described before to afford cbzTris(EG_7SA)$_3$ **18**.

Influenza virus binding studies

Binding of all synthesized sialosides and control molecules to influenza A virus X31 was studied first by an hemagglutination inhibition assay (Table 1). Unfunctionalized core molecules (**1** and **16**), and core molecules carrying only OEG spacers (**24** and **17**) did not show any significant hemagglutination binding inhibition through-out the tested concentration range (Figure 2). Among the adamantane-based compounds, only the trivalent sialoside with EG_6 spacer length, that is, cbzAd(EG_6SA)$_3$ **8** showed inhibition in the micromolar range. This suggests a divalent interaction, which was subsequently validated by synthesizing a divalent sialoside cbzAd(EG_6SA)$_2$ **14**. Binding inhibition values for both cbzAd(EG_6SA)$_3$ **8** and diva-

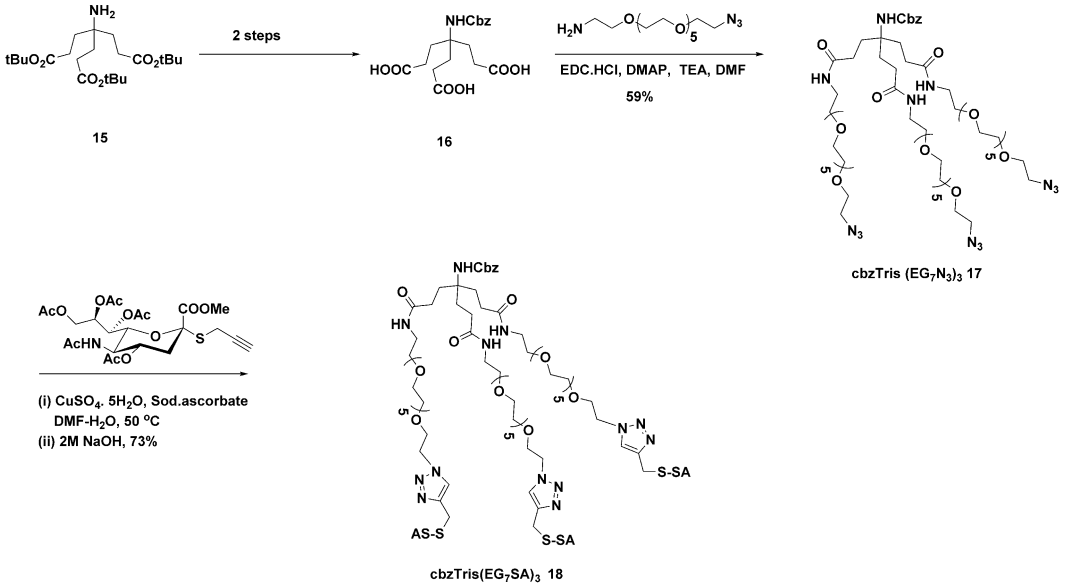

Scheme 5. Synthesis of Tris core trivalent sialosides with an EG_1 and EG_4 spacer.

Table 1. Summary of hemagglutination inhibition values (K_{iHAI}) and apparent dissociation constants ($K_{d,app}$) as determined by microscale thermophoresis (MST).[a]

Compound	K_{iHAI} [mM] SA	K_{iHAI} [mM] tripod	$K_{d,app}$ [μM] tripod
2,6-sialyl lactose	100	–	ND
cbzAd($EG_1SA)_3$ **4**	>20	>6.7	no binding
cbzAd($EG_6SA)_3$ **8**	0.10	0.03	58±15
cbzAd($EG_{14}SA)_3$ **9**	>15	>5	no binding
cbzAd($EG_6SA)_2$ **14**	0.20	0.10	71±11
cbzAd$(COOH)_3$(Control) **1**	no inhibition	>10	no binding
cbzAd($EG_6OH)_3$(Control) **24**	no inhibition	–	no binding
cbzTris($EG_1SA)_3$ **21**	>20	>6.7	169±21
cbzTris($EG_4SA)_3$ **23**	20	6.7	16±4
cbzTris($EG_7SA)_3$ **18**	>50	>16.7	124±21
cbzTris$(COOH)_3$(Control) **16**	no inhibition	–	no binding
cbzTris($EG_7N_3)_3$(Control) **17**	no inhibition	–	no binding

[a] Data from the HAI are given in respect to SA or tripod concentration. For $K_{d,app}$ values the mean ($N \geq 4$) and SEM are given.

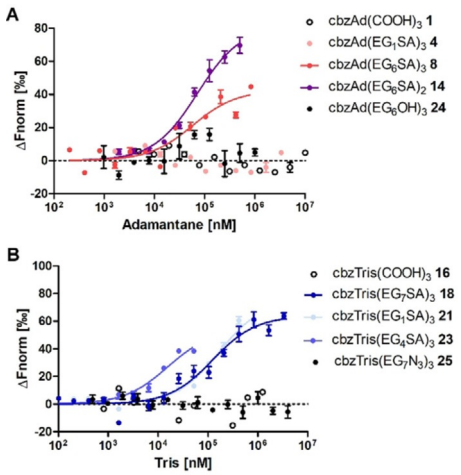

Figure 2. Microscale thermophoresis measurements with intact R18 labeled X31 virus against A) different adamantane-based or B) Tris-based constructs. The change in fluorescence intensity during thermophoresis is shown as a function of the construct's concentration. Data points are one-sited fit. Error bars indicate the SEM ($N \geq 4$).

lent cbzAd($EG_6SA)_2$ **14** were in the micromolar range, i.e., 30 and 100 μM, respectively. The values based on SA are 100 and 200 μM, respectively. The slight difference between both values can be rationalized by the cooperativity factor which is discussed in the next section.

Next, microscale thermophoresis (MST) was applied to determine the affinity constants of all constructs using rhodamine (R18) labeled intact X31 virus. The apparent $K_{d,app}$ values for both trivalent and divalent rigid core-based adamantane sialosides **8** and **14** were almost in the same micromolar range, that is, 58 and 71 μM respectively. Other adamantane based constructs did not show any affinity for the virus which is in agreement with the results from the HAI assay.

The flexible Tris-based core sialosides showed HAI values only in the millimolar range, 6.67 mM was lowest for the one with EG_4 spacer, that is, cbzTris($EG_4SA)_3$ **23.** In contrast, the affinity constant values K_{iHAI} for the Tris core trivalent sialosides measured by MST were in the micromolar range. cbzTris($EG_4SA)_3$ **23** showed enhanced affinity towards virus particles with apparent $K_{d,app}$ around 16 μM. A shorter or longer spacer caused around 10 times lower affinity. The disagreement between the results of HAI and MST measurements might be due to additional non-specific interactions of the compounds with the red blood cells or viral surface at sites other than the sialic acid binding pockets of HA.

Both cores (Ad and Tris) are similar in size. However, the dissociation constant of inhibitor **8** and **23**, which have similar spacer lengths but different cores, differ significantly. We attri-

bute this difference to the flexibility of the inhibitor cores. A binding event is always associated with a restriction of conformational degrees of freedom, which weakens the binding affinity. In case of the more rigid Ad-core, this conformational restriction is less pronounced compared to the more flexible Tris-core, which leads to a stronger binding affinity for Ad-based inhibitors.

Model for trivalent versus divalent binding

The HA inhibition measurements reveal a binding affinity of the trivalent inhibitor **8** that is by about a factor of three stronger than the binding affinity of the divalent inhibitor **14**. To further investigate the size range in which trivalent inhibitors have the potential to outperform their divalent counterparts, we theoretically determined the ratio of the trivalent and divalent dissociation constant in dependence of the average spacer length. The dissociation constant, K_n of *n*-valent ligands that are bound with all *n* binding moieties to an *n*-valent receptor is calculated according to Equation (1):[18]

$$K_n = \frac{K_{mono}^n \omega^n}{C_n} \quad (1)$$

in which each binding moiety, that is, each bound sialic acid, contributes with K_{mono}, the monovalent dissociation constant, to the multivalent dissociation constant. We set K_{mono} = 2.5 mM[19] for the monovalent sialic acid. The angular restriction factor ω accounts for the reduced rotational degrees of freedom due to steric repulsion between the sialic acid and the OEG spacer. The parameter ω describes the angular space available to each sialic acid compared to an unbound monovalent sialic acid unit. We assumed a value of $\omega = 0.03$, which was found for pentavalent inhibitors against cholera toxin and heptavalent inhibitors against the anthrax receptor.[18] The impact of the inhibitor scaffold on the multivalent dissociation constant is quantified by the cooperativity factor C_n, which describes the probability that all *n* sialic acid units are simultaneously bound to the HA receptor. The cooperativity factor accounts for the ligand conformation as well as the number of binding permutations. For both the trivalent as well as the divalent ligand there are six equivalent binding permutations by which the ligands can bind to a trivalent receptor. For the divalent inhibitor, C_n is equivalent to the effective concentration. A detailed discussion of the influence of inhibitor core size and spacer length on the cooperativity factor is presented in the Supporting Information. According to Eq. 1 the ratio between the dissociation constant of a fully bound trivalent and a fully bound divalent inhibitor is obtained from Equation (2):

$$\frac{K_3}{K_2} = K_{mono}\omega\frac{C_2}{C_3} \quad (2)$$

which is shown in Figure 3 depending on the average spacer length r_{ete}. Over a wide range of spacer lengths, the dissociation constant of di- and trivalent inhibitors differ by less than one order of magnitude. While for very short spacers, divalent inhibitors bind stronger than trivalent inhibitors, in the size range of spacer length that is optimal for HA binding, that is, for spacers with a length of around 1.4 nm, the binding affinity of trivalent inhibitors surpasses the divalent inhibitors, due to a favorable binding cooperativity.

Computer simulation studies

To answer the question why only compound **8** exhibited a significant affinity, we set up molecular dynamics simulations of the monovalent counterparts of compounds **8** and **9**. This simulation protocol was chosen in order to minimize computational costs. Still, we were able to determine the behavior of the entire inhibitor, since the extensions of the individual OEG spacers are independent of each other. To trace the conformational behavior of the simulated ligands, we measured the distance distributions for several atom pairs as indicated in Figure 4A. First, we were interested if addition of the OEG spacer influenced the conformational behavior of the adamantane core. As presented in Figure 4B, the C_8—N_5 atom pair distance distributions of both investigated molecules overlapped and were mostly located in the range of 0.7 to 0.9 nm. This finding was not surprising, as the planarity of the amide bond and adjacent triazole ring provided the limited flexibility of this building block. In Figures 4C and 4D, respectively, the distribution of the distance between outermost OEG oxygens, of and the distance between the adamantane core and the sialic acid is shown. Both distributions overlap, but the C_8—S_1 distribution was much narrower, which suggests that the sialic acid and the inhibitor core were in close contact without a receptor, that is, the binding pocket. Therefore, we investigated the formation of the intramolecular hydrogen bonds between all the pairs of hydrogen bond donors and acceptors. Our analysis re-

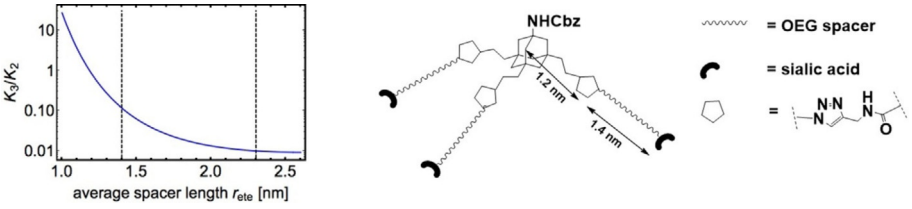

Figure 3. Trivalent versus divalent binding: The ratio of the trivalent dissociation constant K_3 and the divalent dissociation constant K_2, according to Equation (2). The distance between 1.4 nm and 2.3 nm that has to be bridged by the inhibitor spacer to reach HA binding pocket, is indicated by a dashed vertical line.

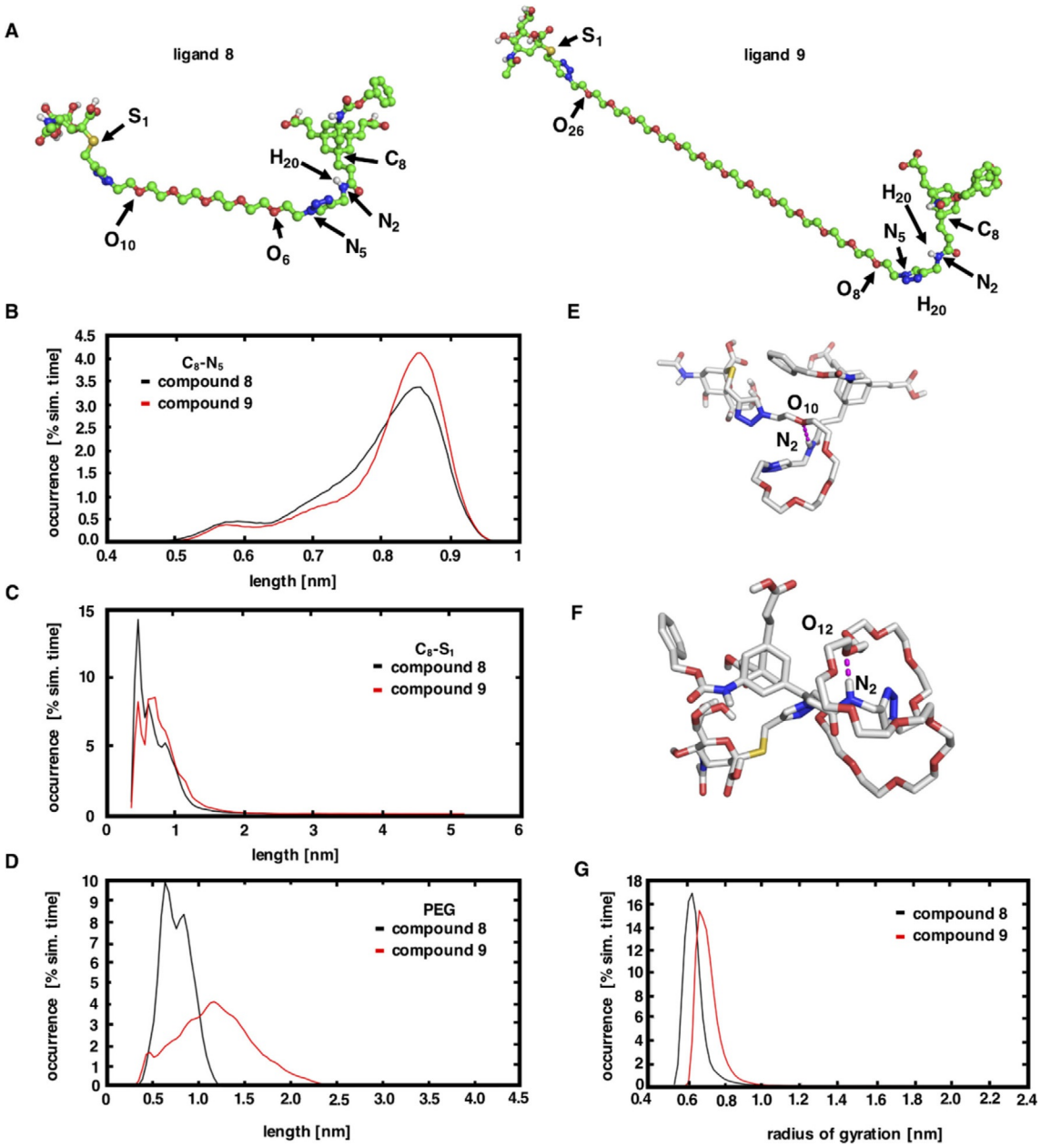

Figure 4. (A) PyMOL representations of the monovalent counterparts of compound **10** (left panel) and compound **11** (right panel). The atoms used to characterize the conformational dynamics of the ligands are marked according to the Acpype parametrization. (B) The distance distribution of the C_8–N_5 atom pair capturing the dynamics of the rigid part of the ligands. (C) The distance distribution of the C_8-S_1 atom pair capturing the distance between the rigid core and sialic acid. (D) The distance distribution of the outermost oxygen atoms of OEG spacers. (E) PyMOL representation of the most stable intramolecular hydrogen bond of compound **8**. (F) PyMOL representation of the most stable intramolecular hydrogen bond of compound **9**. (G) Distribution of the radius of gyration compounds **8** and **9**.

vealed that sialic acid remained free to potentially interact with the respective binding site of HA. In both simulated systems, the bonded atom pair N_2–H_{20} was the most dominant hydrogen bond donor. It holds the OEG spacer and imidazole ring adjacent to the sialic acid in proximity to the adamantane core through the formation of several transient hydrogen bonds. In the case of compound **8**, N_2–H_{20} donor participated in the intramolecular hydrogen bonding for 34.5% of the simulation time, whereas it acted for compound **9** for the half of the simulation time. These findings would suggest that these two compounds should have bound to HA with almost similar affinity. Intuitively one notices from Figures 4E and 4G the increase in the length of OEG spacer is correlated with the increase in the size of the respective OEG coil. To quantify the size of OEG coils, we used the radius of gyration as a measure. As shown in Figure 4G, the size of OEG coils of compound **9** is indeed larger compared to compound **8**. If we now consider that all three OEG arms adopted the OEG-coil conformation, then the whole molecule would have been in a rather globular/compact conformation resulting in steric repulsion from the

receptor. Having the larger overall size of the OEG-coils, long spacer inhibitor **9** would repel more often from the surface of the receptor, thus the probability for the binding event is reduced compared to short spacer inhibitor **8**.

Consequently, this suggests that compound **8** unfolds from the coil-like structure easier than compound **9**, which might explain the inhibitory constant in the micromolar range.

Conclusions

We have presented a quantitative comparison of the rigid and flexible core trivalent sialosides for influenza virus inhibition. The rigid adamantane core trivalent sialoside with hexamethylene glycol spacer is the most potent candidate against IAV/X31, showing an inhibitory constant in the micromolar range. On the contrary, no binding was observed with a longer OEG spacer, which is consistent with the simulation data that suggests increased conformational penalties when the OEG length is increased from EG_6 to EG_{14}. We also observed that trivalent cbzAd(EG_6SA)$_3$ **4** ($K_i = 30$ μM) was slightly more potent than the divalent cbzAd(EG_6SA)$_2$ **14** (Ki = 100 μM) in the HAI assay, which could be assigned to a somewhat higher rebinding probability for the trivalent sialoside. However, both binding constants indicate a bivalent binding between ligand and receptor. Flexible Tris core-based systems did not show any potent inhibitions in the HAI assay. The observed micromolar range affinity constant values in MST for the Tris core sialosides might be assigned to an interaction other than HA with the virus particles. Following, non-specific interaction of Tris-based compounds with cell membranes or binding to virus structures other than HA needs to be further investigated. Overall, our findings show that optimizing a significantly active trivalent sialoside with a non-toxic and structurally simple spacer like OEG is a challenging task because of high conformational entropic penalties and the chance of intramolecular hydrogen bonding with the spacer groups on the core itself. Nevertheless, we could design an adamantane-based trivalent sialoside which was significantly more active in the HAI assay compared to monovalent SA or other adamantane derivatives used in this study. Trivalent cluster units, such as cbzAd(EG_6SA)$_3$, could be further used for a multimeric presentation on larger scaffolds to achieve even better inhibition constants against the influenza A virus.

Experimental Section

Synthesis

All reagents and solvents were purchased from commercial suppliers and used without further purification. Analytical grade PEG600 ($\approx EG_{14}OH$), hexa-, tetraethylene glycol, and azido-amino EG_7 were purchased from Fischer Chemical, Sigma Aldrich, Acros Organic, and Polypure, respectively. Reactions requiring dry or oxygen-free conditions were carried out under argon in Schlenk glassware. ^1H and ^{13}C NMR spectra were recorded on Bruker AMX 500 (500 and 125 MHz for ^1H and ^{13}C NMR, respectively) and Delta Joel Eclipse 700 (700 and 175 MHz for ^1H and ^{13}C NMR, respectively) spectrometer at 25 °C and calibrated by using the deuterated solvent peak. Infrared (IR) spectra were recorded with a Nicolet AVATAR 320 FT-IR 5 SXC (Thermo Fisher Scientific, Waltham, MA, USA) with a DTGS detector from 4000 to 650 cm^{-1}. A TSQ 7000 (Finnigan Mat) instrument was used for ESI measurements and a JEOL JMS-SX-102A spectrometer was used for the high-resolution mass spectra. Naturally occurring sialic acids constitute a family of more than 50 structurally distinct nine-carbon 3-deoxy-ulosonic acids, the most widespread derivative being 5-*N*-acetyl-neuraminic acid (Neu5Ac) was used as starting material for the preparation of prop-2-ynyl α-thiosialoside. We used the abbreviation of sialic acid (SA) for Neu5Ac. Similarly 'Tris' was used as an abbreviation for the commercially available 4-(((benzyloxy)carbonyl)amino)-4-(2-carboxyethyl)heptanedioic acid based flexible core.

Biological assay

Virus material: X31 virus (influenza strain A/Aichi/2/68 H3N2) was harvested from allantoic fluid of embryonated chicken eggs. Virus isolates were clarified upon low speed centrifugation (300×*g*, 10 min). For binding (inhibition) experiments clarified allantoic fluid was further concentrated by ultracentrifugation (100 000×*g*, 1 h).

Synthesis and characterization cbzAd(CH_2CH_2NHS)$_3$ 2

cbzAd(CH_2CH_2COOH)$_3$ **1**[17] (510 mg,1 mmol), EDC·HCl (868 mg, 4.5 mmol) and NHS-OH (520 mg, 4.5 mmol) were dissolved in 20 mL abs. DMF and stirred for 12 h at rt. The solvent was removed in vacuo and the residue was dissolved in 50 mL EtOAc. The solution was washed with water (3×50 mL), dried over Na_2SO_4, and filtered. The solvent was removed in vacuo and the residue recrystallized from PrOH to give the title compound **2** (729 mg, 92%) as a colorless solid. ^1H NMR (600 MHz, $CDCl_3$): δ (ppm) = 7.39–7.29 (m, 5H, aryl H), 5.04 (s, 2H, benzyl H), 4.87 (s, 1H, -NH-), 2.82 (br s, 12H, 9-H), 2.60 (t, 6H, ^3J = 7.6 Hz, 6-H), 1.70 (t, 6H, ^3J = 7.6 Hz, 5-H), 1.64 (s, 6H, 2-H), 1.22 (d, 3H, ^2J = 12.0 Hz, 4-Ha), 1.14 (d, 3H, ^2J = 12.0 Hz, 4-He); ^{13}C NMR (150 MHz, $CDCl_3$): δ (ppm) = 169.3, 169.2, 154.8, 136.9, 128.7, 128.2, 128.2, 66.3, 52.7, 44.8, 44.8, 36.8, 35.2, 25.7, 25.3; IR (film): ν = 2974, 2860, 1724, 1460, 1070, 910 cm^{-1}; HRMS (ESI) = *m/z* calcd for $C_{39}H_{44}N_4O_{14}$: 793.2927 [$M+H^+$], found 793.2925.

cbzAd(CH_2CH_2SA)$_3$ 4

O-Benzyloxycarbonylaminoethoxy sialic acid **3** (166 mg, 0.33 mmol) was dissolved in 5 mL H_2O/MeOH (v/v = 1/4) and treated with LiOH (26 mg, 1.10 mmol). The solution was stirred at rt for 2 h and neutralized with Amberlite IR-120. After filtration, the solution was freeze dried and the residue was dissolved in 20 mL MeOH/H_2O (v:v = 1:1). The solution was treated with 10 mg Pd/C under H_2-atmosphere (balloon) and stirred for 24 h at rt. After filtration, the solvent was removed in vacuo and the residue was dissolved in abs. DMSO and treated with NEt_3 (50 μL, 0.36 mmol). To this solution, NHS-ester **2** (75 mg, 0.09 mmol) was added and the mixture was stirred for 48 h at rt. The solvent was removed in vacuo and the crude product was purified by column chromatography on RP-18 silica (H_2O/MeCN 1:0–0:1). The title compound **4** (37 mg, 35%) was obtained as a colorless solid. ^1H NMR (600 MHz, D_2O): δ (ppm) = 7.47–7.37 (m, 5H, aryl H), 5.07 (s, 2H, benzyl H), 3.89–3.78 (m, 12H, 18-H, 16-H, 14-H), 3.72–3.66 (m, 6H, 13-H, 17-H), 3.64 (td, 3H, ^2J = 10.1 Hz, ^3J = 5.1 Hz, 9-Ha), 3.58 (br d, 3H, ^3J = 9.2 Hz, 15-H), 3.51 (td, 3H, ^2J = 10.1 Hz, ^3J = 5.1 Hz, 9-Ha), 3.36–3.31 (m, 6H, 8-H), 2.73 (dd, 3H, ^2J = 12.3 Hz, ^3J = 4.8 Hz, 12-He), 2.22 (br s, 6H, 6-H), 2.03 (s, 9H, -$NHCOCH_3$), 1.68 (dd, 3H, ^2J = 12.3 Hz, ^3J = 12.3 Hz, 12-Ha), 1.54 (s, 6H, 2-H), 1.49 (br s, 6H, 5-H), 1.17 (d, 3H, ^2J = 12.0 Hz,

4-Ha), 1.11 (d, 3H, ^2J=12.0 Hz, 4-Hb); ^{13}C NMR (150 MHz, D_2O): δ (ppm)=177.8, 175.1, 173.6, 136.7, 128.8, 128.2, 127.6, 100.5, 72.6, 71.6, 68.2, 68.2, 66.3, 62.64, 62.61, 52.9, 51.9, 44.3, 44.1, 40.2, 39.4, 38.4, 34.6, 30.0, 22.0; IR (film): ν=2920, 1751, 1670, 1527, 1369, 1226, 1076, 1039, 848 cm^{-1}; HRMS (ESI): *m/z* calcd for $C_{66}H_{101}N_7O_{32}$: 1504.6564 [$M+H^+$], found 1504.6535.

Synthesis of the compound cbzAd(propargyl)$_3$ 5

cbz-Adamantane triacid **1** (0.7 g, 1.4 mmol) was dissolved in dry DMF (100 mL) and cooled to 0 °C (ice bath). DIPEA (0.9 mL, 5.3 mmol) was added to the reaction mixture and stirred for 5 min followed by addition of EDC·HCl (1.0 g, 5.3 mmol) and HOBt (0.7 g, 5.3 mmol). The reaction mixture was stirred for 30 min. Then propargyl amine (0.3 mL, 5.3 mmol) was added and stirred for 72 h at room temperature. DMF was removed and the residue was dissolved in ethyl acetate (250 mL) and washed with 1 M HCl (3× 100 mL), water (100 mL), and brine (2×50 mL). The organic phase was dried over Na_2SO_4, and the solvent was removed under reduced pressure. The resulting crude product was purified by flash chromatography on silica gel ($CHCl_3$/methanol) to afford the propargylated product **5** (453.68 mg, 53%).^{1}H NMR (400 MHz, CD_3OD): δ (ppm)=7.34–7.26 (m, 5H, aryl H), 5.01 (s, 2H, benzyl H), 3.93 (d, 6H, ^4J=4.0 Hz, -NHCO*CH*$_2$CCH), 2.57 (t, 3H, ^4J=4.0 Hz, -NHCOCH$_2$C*CH*), 2.17 (t, 6H, ^3J=4.0 Hz, AdCH$_2$*CH*$_2$CONH-), 1.58 (s, 6H, AdH), 1.49 (t, 6H, ^3J=8.0 Hz, Ad*CH*$_2$CH$_2$CONH-), 1.19–1.09 (m, 6H, AdH); ^{13}C NMR (100 MHz, CD_3OD): δ (ppm)=176.2, 153.4, 138.6, 129.4, 128.9, 128.7, 80.7, 72.1, 53.7, 46.3, 45.9, 39.7, 36.1, 30.8, 29.4; IR (film): ν=3282, 2913, 1645, 1529, 1454, 1420, 1385, 1353, 1307, 1235, 1024 cm^{-1}; HRMS (ESI)=*m/z* calcd for $C_{36}H_{44}N_4O_5$.635.3209 [$M+Na^+$]; found: 635.3200.

Synthesis of the compound cbzAd(EG$_6$N$_3$)$_3$ 6 and cbzAd(EG$_{14}$N$_3$)$_3$ 7

The cbz protected adamantane (propargyl)$_3$ **5** (50.0 mg, 0.081 mmol) and N_3EG_6OTs (Scheme S3) (188.0 mg, 0.041 mmol) was dissolved in DMF (10 mL). $CuSO_4$·5H_2O (12.2 mg, 0.048 mmol) was dissolved in 0.2 mL of H_2O and added to the solution of sodium ascorbate (97.2 mg, 0.48 mmol) in 0.4 mL H_2O. The resultant solution of salts in water was added drop wise to the solution containing cbzAd(propargyl)$_3$ **5** and N_3EG_6OTs. The reaction mixture was degassed with argon for 10 minutes and then allowed to stir at room temperature for 48 h. The completion of reaction was monitored by checking TLC and ESI. HRMS(ESI)=*m/z* calcd for $C_{93}H_{137}N_{13}O_{26}S_3$: 2019.8739 [$M+Na^+$]; found: 2019.8884 to ensure the reaction completion. It was followed by in situ azidation with NaN_3 (31.8 mg, 0.489 mmol), at 70 °C for 24 h. The stirring was stopped, and solvent was removed under reduced pressure. Reaction mixture was first filtered through Celite and washed with $CHCl_3$ to remove excess of DMF. The organic solvent was evaporated. The crude product was purified by flash column chromatography on silica gel ($CHCl_3$/MeOH) to afford the pure product as colorless oil (65.0 mg, 50%).

cbzAd(EG$_6$N$_3$)$_3$ 6

^{1}H NMR (500 MHz, $CDCl_3$): δ (ppm)=7.69 (s, 3H, -C=CH-), 7.32–7.28 (br m, 4H, aryl H), 6.92 (s, 1H, aryl H), 4.96 (s, 2H, benzyl H), 4.47 (t, 6H, J=10 Hz, -TrzCH$_2$*CH*$_2$O-), 4.44 (d, 6H, J=10 Hz, -NH*CH*$_2$Trz-), 3.81 (t, 6H, J=10 Hz, -TrzCH$_2$*CH*$_2$O-), 3.64–3.57 (m, 66H, -O*CH*$_2$CH$_2$N$_3$, EG spacer), 3.35 (t, 6H, J=10 Hz, -O*CH*$_2$CH$_2$N$_3$), 2.08 (t, 6H, J=10 Hz, AdCH$_2$*CH*$_2$CONH-), 1.47–1.44 (br m, 12H, AdH and Ad*CH*$_2$CH$_2$CONH-), 1.06–0.94 (br m, 6H, AdH); ^{13}C NMR (125 MHz, $CDCl_3$): δ (ppm)=173.4, 154.4, 144.6, 136.7, 128.5, 128.0, 123.4, 70.5, 70.0, 69.4, 65.9, 52.7, 50.6, 50.2, 45.1, 38.0, 34.9, 30.1, 29.6, 22.8; IR (film): ν=3301, 2906, 2360, 2105, 1715, 1654, 1540, 1455, 1349, 1302, 1242, 1117, 940, 736 cm^{-1}; HRMS (ESI)=*m/z* calcd for $C_{72}H_{116}N_{22}O_{20}$: 1631.8634 [$M+Na^+$]; found: 1631.8717.

cbzAd(EG$_{14}$N$_3$)$_3$ 7

Synthesis was carried out by the above-reported procedure. The crude product was purified by dialysis with MWCO 2 kDa in $CHCl_3$ to afford the pure product as colorless oil (125.77 mg, 58.5%), ^{1}H NMR (500 MHz, CD_3OD-CD_2Cl_2): δ (ppm)=7.75 (s, 3H, -C=CH-), 7.26 (br s, 4H, aryl H), 7.13 (s, 1H, aryl H), 4.94 (s, 2H, benzyl H), 4.90–4.47 (br m, 12H, -TrzCH$_2$*CH*$_2$O- and -NH*CH*$_2$Trz-), 4.35 (s, 6H, -TrzCH$_2$*CH*$_2$O-), 3.81 (s, 6H, -O*CH*$_2$CH$_2$N$_3$), 3.58–3.33 (m, 156H, -O*CH*$_2$CH$_2$N$_3$, EG spacer), 1.49–1.43 (m, 12H, AdH and Ad*CH*$_2$CH$_2$CONH-), 1.10–1.01 (br m, 6H, AdH); ^{13}C NMR (125 MHz, $CDCl_3$): δ (ppm)=173.5, 154.5, 144.7, 136.6, 128.6, 128.1, 123.5, 70.6, 70.1, 69.4, 66.0, 52.8, 50.7, 50.3, 45.3, 38.1, 35.0, 34.1, 29.7, 22.9; IR (film): ν=3318, 2910, 2868, 2103, 1769, 1717, 1651, 1534, 1455, 1349, 1283, 1240, 1113, 1035, 992, 932, 841, 777 cm^{-1}; HRMS (ESI)=*m/z* calcd for $C_{120}H_{212}N_{22}O_{44}$: 2705.4698 [$M+K^+$]; found: 2705.4340.

Synthesis of cbzAd(EG$_6$SA)$_3$ 8 and cbzAd(EG$_{14}$SA)$_3$ 9

cbzAd(EG$_6$SA)$_3$ 8: cbzAd(EG$_6$N$_3$)$_3$ **6** (0.05 g, 0.03 mmol) and prop-2-ynyl α-thiosialoside (0.06 g, 0.11 mmol) was dissolved in DMF (5 mL). The $CuSO_4$·5H_2O (0.77 mg, 0.003 mmol) was dissolved in 0.2 mL of H_2O and added to the solution of sodium ascorbate (6.2 mg, 0.03 mmol) in 0.4 mL H_2O. The resultant solution of salts in water was added drop wise to the solution containing cbzAd(EG$_6$N$_3$)$_3$ **6** and prop-2-ynyl α-thiosialoside. The reaction mixture was degassed with argon for 10 minutes and then allowed to stir at room temperature for 48 h. The completion of reaction was monitored by IR for the disappearance of the N_3 frequency at 2100 cm^{-1}. After the reaction completion, DMF was evaporated over a rota-vapor. Then 2 M NaOH (5 mL) solution was added to the left-over residue and stirred for 2 h at room temperature. The solution was dialyzed against water for 3 days using dialysis membrane with MWCO 2 kDa to afford the pure product as white solid (70.56 mg, 84%). ^{1}H NMR (700 MHz, D_2O): δ (ppm)=7.87 (s, 3H, -C=CH-), 7.26 (br s, 5H, aryl H), 4.91 (s, 2H, benzyl H), 4.49 (br s, 12H, -TrzCH$_2$*CH*$_2$O- and -OCH$_2$*CH*$_2$Trz-), 4.34 (br s, 6H, -NH*CH*$_2$Trz-), 3.95–3.48 [m, 87H, -TrzCH$_2$*CH*$_2$O-, -OCH$_2$*CH*$_2$Trz-, SA (8-H, NH, 7-H, 4-H, 9-H, 5-H, 6-H), SCH$_2$C=C, EG spacer], 2.72 (d, 3H, J=7 Hz, SA H-3e), 2.10 (br s, 6H, AdCH$_2$*CH*$_2$CONH-), 1.94 (s, 3H, SA NHAc), 1.69 (s, 3H, SA H-3a), 1.35 (br s, 12H, AdH and Ad*CH*$_2$CH$_2$CONH-), 0.94 (br s, 6H, AdH); ^{13}C NMR (175 MHz, D_2O): δ (ppm)=177.0 175.1, 156.0, 145.0, 136.6, 128.7, 128.2, 127.6, 124.8, 124.5, 74.8, 71.7, 69.5, 68.7, 68.7, 68.5, 68.1, 65.9, 62.5, 52.6, 51.7, 50.0, 44.3, 44.2, 40.6, 38.0, 34.6, 34.4, 29.9, 23.5, 22.0; IR (film): ν=3268, 2915, 1644, 1608, 1550, 1372, 1133, 1028, 951, 834 cm^{-1}; HRMS (ESI)=*m/z* calcd for $C_{114}H_{179}N_{25}O_{44}S_3$: 2721.1553 [$M+Na^+-H^+$], found: 2721.1324; calcd 2737.1292 [$M+K^+-H^+$], found: 2731.1120.

cbzAd(EG$_{14}$SA)$_3$ 9: Synthesis was carried out by the above-reported procedure. The crude product was purified by dialysis with MWCO 2 kDa in $CHCl_3$ to afford the pure product as colorless oil (69.83 mg, 62%). ^{1}H NMR (700 MHz, D_2O): δ (ppm)=7.97 (s, 3H, -C=CH-), 7.36 (br s, 5H, aryl H), 5.02 (s, 2H, benzyl H), 4.57 (br s, 12H, -TrzCH$_2$*CH*$_2$O- and -OCH$_2$*CH*$_2$Trz-), 4.41 (br s, 6H, -NH*CH*$_2$Trz-), 4.04–3.52 [m, 180H, -TrzCH$_2$*CH*$_2$O-, -OCH$_2$*CH*$_2$Trz-, SA (8-H, 7-H, 4-H, 9-H, 5-H, 6-H), SCH$_2$C=C, EG spacer], 2.79 (d, 3H, J=7 Hz, SA H-3e), 2.18–2.16 (br m, 6H, AdCH$_2$*CH*$_2$CONH-), 2.01 (s, 3H, SA NHAc), 1.77

(s, 3H, SA H-3a), 1.44–142 (m, 12H, AdH and AdCH_2CH_2CONH-), 1.05–0.99 (br m, 6H, AdH); ^{13}C NMR (175 MHz, D_2O): δ (ppm) = 177.0, 175.1, 156.0, 145.0, 136.6, 128.7, 128.2, 127.6, 124.8, 124.5, 74.8, 71.7, 69.5, 68.7, 68.7, 68.5, 68.1, 65.9, 62.5, 52.6, 51.7, 50.0, 44.3, 44.2, 40.6, 38.0, 34.6, 34.4, 29.9, 23.5, 22.0; *m/z* calcd for $C_{162}H_{272}N_{25}NaO_{68}S_3$: 3777.79 [$M+Na^+$]; GPC ($H_2O$): Mn = 4071 Da, Mw = 4756 kDa, PDI = 1.16; Elemental analysis: calcd 51.79% C, 7.38% H, 9.32% N, 2.56% S, found. 51.62% C, 7.40% H, 9.29% N, 2.60% S. IR (film): ν = 3274, 2872, 1607, 1549, 1454, 1350, 1245, 1080, 950, 892, 834 cm^{-1}.

Synthesis of the compound cbzAd(COOH)$_2$ 11

Bis(2-carboxyethyl) aminoadamantane **10** (2 g, 6.78 mmol) was dissolved in dioxane (30 mL) followed by addition of aqueous $NaHCO_3$ (850 mg, 10.12 mmol, 30 mL) solution. NaOH (2 M) was added to the reaction mixture to achieve the pH of 9 and the reaction mixture was cooled to 0 °C (ice bath). Benzyl chloroformate (1.73 mL, 12.10 mmol) was added dropwise to the stirred solution. Stirring was continued at room temperature overnight. The reaction mixture was washed three times with CH_2Cl_2 (30 mL) and three times with EtOAc (30 mL), acidified to pH 1, and extracted six times with EtOAc. The combined organic layers were dried over Na_2SO_4, filtered, and concentrated to give the intermediate cbz-protected diacid (1.78 g, 62%). ^{1}H NMR (500 MHz, $CDCl_3$): δ (ppm) = 7.37–7.31 (m, 5H, aryl H), 5.04 (s, 2H, benzyl H), 2.30 (t, 4H, ^3J = 10 Hz, 9′-H), 2.20 (br t, 1H, 6′-H), 1.80 (br. s, 2H, 7′-H), 1.65–1.58 (m, 4H, 2′-H), 1.53 (t, 4H, ^3J = 10 Hz, 8′-H), 1.39–1.32 (m, 4H, 5′-H), 1.15 (br s, 2H, 4′-H); ^{13}C NMR (125 MHz, $CDCl_3$): δ (ppm) = 179.7, 128.6, 128.2, 45.6, 40.4, 37.5, 34.7, 29.6, 28.1; IR (film): ν = 3032, 2915, 2850, 1704, 1587, 1497, 1454, 1392, 1341, 1302, 1261, 1025, 941, 909, 823, 788 cm^{-1}; HRMS (ESI) = *m/z* calcd for $C_{24}H_{31}NO_6$:452.2049 [$M+Na^+$]; found: 452.2083.

Synthesis of the compound cbzAd(propargyl)$_2$ 12

cbz-protected diacid **11** (350 mg, 0.82 mmol) was dissolved in 15 mL dry DMF and cooled to 0 °C (ice bath). Then DCC (336 mg, 1.63 mmol) and *N*-hydroxysuccinimide (196 mg, 1.70 mmol) were added, and the reaction mixture was stirred at room temperature for 12 h. The completion of reaction was monitored by mass spectrometry. Then propargyl amine (0.14 mL, 2.18 mmol) was added and stirred for 72 h at rt. The solution was diluted with ethyl acetate (70 mL) and washed with 1 M HCl (3×20 mL), water (40 mL), and brine (2×20 mL). The organic phase was dried over Na_2SO_4, and the solvent was removed under reduced pressure. The crude product was purified by column chromatography with a DCM/methanol mixture. (233.18 mg, 57%). ^{1}H NMR (700 MHz, CD_3OD): δ (ppm) = 7.33–7.26 (m, 5H, aryl H), 4.99 (s, 2H, benzyl H), 3.91 (d, 4H, ^4J = 7 Hz, 11′-H), 2.34 (t, 2H, ^4J = 7 Hz, 12′-H), 2.16–2.12 (m, 5H, 9′-H, 6′-H), 1.79 (br s, 2H, 7′-H), 1.62–1.55 (m, 4H, 2′-H), 1.48–1.44 (m, 4H, 8′-H), 1.39–1.29 (m, 4H, 5′-H); 1.14 (br s, 2H, 4′-H); ^{13}C NMR (175 MHz, CD_3OD): δ (ppm) = 175.5, 128.9, 128.5, 128.2, 80.0, 71.5, 52.6, 46.1, 45.8, 40.9, 39.2, 35.2, 30.3, 29.2; IR (film): ν = 3288, 3060, 2910, 2847, 2358, 1701, 1646, 1536, 1454, 1420, 1343, 1301, 1235, 1138, 1113, 1045, 1031, 928, 736, 697 cm^{-1}; HRMS (ESI) = *m/z* calcd for $C_{30}H_{37}N_3O_4$:527.2682 [$M+1+Na^+$]; found: 527.2755.

Synthesis of the compound SAEG$_6$N$_3$ 13

$TsEG_6N_3$ was synthesized from EG_6 diol. The $TsEG_6N_3$ (500 mg, 1.08 mmol) and prop-2-ynyl α-thiosialoside (914 mg, 1.68 mmol) were dissolved in DMF. $CuSO_4$·5H_2O (0.06 mg, 0.24 mmol) was dissolved in 0.2 mL of H_2O and added to the solution of sodium ascorbate (511 mg, 2.57 mmol) in 0.4 mL H_2O. The resultant solution of salts in water was added drop wise to the solution containing $TsEG_6N_3$ and prop-2-ynyl α-thiosialoside. The reaction mixture was degassed with argon for 10 minutes and then allowed to stir at 40 °C for 48 h. The completion of reaction was monitored by IR spectroscopy for the disappearance of azide peak. It was followed by in situ azidation with NaN_3 (716 mg, 11.02 mmol), at 70 °C for 24 h. The stirring was stopped, and solvent was removed under reduced pressure. The crude compound was purified by column chromatography to obtain the pure product **SAEG$_6$N$_3$ 13**. (691.40 mg, 73%). ^{1}H NMR (500 MHz, CD_2Cl_2): δ (ppm) = 7.66 (s, 1H, -C=CH-), 5.59 (m, 1H, 8-H), 5.43–5.39 (m, 1H, 7-H), 4.91–4.86 (m, 1H, 4-H), 4.49 (t, J = 10 Hz, 2H, -TrzCH_2CH_2O-), 4.27 (dd, 1H, ^2J = 10 Hz, ^3J = 5 Hz, 9-Ha), 4.09–3.98 (m, 4H, 5-H, 9-He, -SCH_2C=CH-), 3.92–3.88 (m, 2H, 6-H, 5-H), 3.85 (t, 2H, -TrzCH_2CH_2O-), 3.71 (s, 3H, -OCH_3), 3.65–3.57 (m, 18H, EG spacer), 3.36 (t, 2H, ^3J = 5 Hz, -$CH_2CH_2N_3$-), 2.74 (dd, 1H, ^2J = 10 Hz, ^3J = 5 Hz, 3-He), 2.14 (s, 3H, -OCOCH_3), 2.11 (s, 3H, -OCOCH_3), 1.99 (s, 3H, -OCOCH_3), 1.98 (s, 3H, -OCOCH_3), 1.83 (s, 3H, -NHOCH_3); ^{13}C NMR (500 MHz, CD_2Cl_2): δ (ppm) = 171.0, 170.9, 170.5, 170.3, 168.7, 143.5, 123.9, 83.5, 74.5, 71.0, 71.0, 71.0, 70.9, 70.8, 70.3, 69.9, 68.6, 67.9, 62.7, 53.5, 51.2, 50.7, 49.5, 38.1, 23.8, 23.4, 21.5, 21.1, 21.1, 21.0; IR (film): ν = 3274, 2869, 2103, 1736, 1682, 1662, 1543, 1437, 1368, 1215, 1121, 1032, 946 cm^{-1}; HRMS (ESI) = *m/z* calcd for $C_{35}H_{55}N_7O_{17}S$: 900.3273 [$M+Na^+$]; found: 900.3270.

Synthesis of the compound cbzAd(EG$_6$SA)$_2$ 14

The $SAEG_6N_3$ (174 mg, 0.20 mmol) and cbzAd(propargyl)$_2$ **12** (50 mg, 0.099 mmol) were dissolved in DMF, $CuSO_4$·5H_2O (9.9 mg, 0.03 mmol) was dissolved in 0.2 mL of H_2O and added to the solution of sodium ascorbate (78 mg, 0.39 mmol) in 0.4 mL H_2O. The resultant solution of salts in water was added drop wise to the solution containing $SAEG_6N_3$ and cbzAd(propargyl)$_2$. The reaction mixture was degassed with argon for 10 minutes and then allowed to stir at 40 °C for 48 h. The completion of reaction was monitored by IR spectroscopy for the disappearance of azide peak. The stirring was stopped, and solvent was removed under reduced pressure. 2 M NaOH (20 mL) was added to the residue and stirred at room temperature for 12 h. The reaction mixture was dialyzed first against water and aqueous EDTA solution for 2 days and again using only water for 4 days. The aqueous solution obtained after dialysis was lyophilized to get the pure product cbzAd(EG$_6$SA)$_2$ **14** (146.24 mg, 78%). ^{1}H NMR (700 MHz, D_2O): δ (ppm) = 8.30 (br s, 4H, -C=CH-), 7.41–7.38 (m, 5H, aryl H), 5.04 (s, 2H, benzyl H), 4.65–4.62 (m, 4H, -TrzCH_2CH_2O- and -OCH_2CH_2Trz-), 4.47 (br s, 4H, -NHCH_2Trz-), 3.98–3.49 [m, 56H, -TrzCH_2CH_2O-, -OCH_2CH_2Trz-, SA (8-H, 7-H, 4-H, 9-H, 5-H, 6-H), SCH_2C=C, EG spacer], 2.89 (br s, 2H, SA H-3e), 2.28 (br s, 4H, AdCH_2CH_2CONH-), 2.13 (br s, 1H, 6′-H), 2.04 (s, 6H, SA NHAc), 1.73 (br s, 2H, Ad 7′-H), 1.54–1.48 (m, 8H, Ad 2′-H, AdCH_2CH_2CONH-), 1.28 (br d, 4H, Ad 5′-H), 1.11 (br s, 2H, Ad 4′-H); ^{13}C NMR (175 MHz, D_2O): δ (ppm) = 177.0, 174.9, 156.0, 136.9, 128.7, 128.2, 127.6, 74.8, 71.8, 69.5, 68.5, 68.1, 62.4, 51.6, 50.4, 44.7, 40.6, 39.5, 38.3, 34.3, 29.2, 22.0; IR (film): ν = 3279, 2905, 2360, 1698, 1614, 1551, 1428, 1349, 1235, 1109, 1023, 948, 890, 834 cm^{-1}; HRMS (ESI) = *m/z* calcd for $C_{82}H_{127}N_{17}O_{30}S_2$: 1915.8274 [$M+Na^+-1$]; found: 1915.8152.

Synthesis of the compound cbzTris(EG$_7$N$_3$)$_3$ 17

cbz-protected triacid **16** (231 mg, 0.61 mmol) was dissolved in 15 mL of dry DMF and cooled to 0 °C (ice bath). Then triethylamine (0.35 mL, 2.51 mmol), EDC·HCl (493 mg, 2.57 mmol) and DMAP (169 mg, 1.38 mmol) were added, and the reaction mixture was

stirred at 0 °C for 20 minutes. Then $N_3EG_7NH_2$ (902 mg, 2.58 mmol) was added and stirred at room temperature for 72 h. The solution was diluted with ethyl acetate (70 mL) and washed with 1 M HCl (3×20 mL), water (40 mL), and brine (2×20 mL). The organic phase was dried over Na_2SO_4, and the solvent was removed under reduced pressure. The crude product was purified by column chromatography with a DCM/methanol mixture to afford the pure **cbzTris(EG_7N_3)$_3$ 17** (49.55 mg, 59%). ^{1}H NMR (500 MHz, [D_6]DMSO): δ (ppm) = 7.87 (t, ^3J = 5 Hz, 3H,- N*H*CH_2CH_2-), 7.34–7.29 (m, 5H, aryl H), 4.97 (s, 2H, benzyl H), 3.60 (t, ^3J = 5 Hz, 6H, -NHC*H*$_2$$CH_2$-), 3.54–3.50 (m, 60H, EG spacer), 3.39 (t, ^3J = 5 Hz, 12H, -NHCH_2C*H*$_2$, -C*H*$_2$$CH_2N_3$-), 3.18–3.16 (m, 6H, -$CH_2$C*H*$_2$$N_3$-), 2.01 (t, ^3J = 10 Hz, 6H,—CH_2C*H*$_2$CONH-); 1.76 (br t, 6H, -C*H*$_2$$CH_2$CONH-); ^{13}C NMR (125 MHz, [D_6]DMSO): δ (ppm) = 172.1, 154.1, 137.3, 128.3, 127.4, 69.7–69.1, 64.5, 56.1, 50.0, 30.3, 29.5; IR (film): ν = 3301, 2921, 2868, 2106, 1717, 1650, 1533, 1455, 1348, 935, 746 cm^{-1}; HRMS (ESI): *m/z*: calcd for $C_{60}H_{107}N_{13}O_{23}$: 1400.7500 [$M+Na^+$]; found 1400.7518.

Synthesis of the compound cbzTris(EG_7SA)$_3$ 18

The prop-2-ynyl α-thiosialoside (154 mg, 0.42 mmol) and cbzTris(EG_7N_3)$_3$ (100 mg, 0.07 mmol) were dissolved in DMF. $CuSO_4$·5H_2O (21 mg, 0.08 mmol) was dissolved in 0.2 mL of H_2O and added to the solution of sodium ascorbate (217 mg, 1.10 mmol) in 0.4 mL H_2O. The resultant solution of salts in water was added drop wise to the solution containing prop-2-ynyl α-thiosialoside and cbzTris(EG_7N_3). The reaction mixture was degassed with argon for 10 minutes and then allowed to stir at 40 °C for 48 h. The completion of reaction was monitored by IR spectroscopy for the disappearance of azide peak. The stirring was stopped, and solvent was removed under reduced pressure 2 M NaOH (20 mL) was added to the residue and stirred at room temperature for 12 h. The reaction mixture was dialyzed against water and aqueous EDTA solution. The aqueous solution obtained after dialysis was lyophilized to get the pure product cbzTris(EG_7SA)$_3$ **18**. (125.85 mg, 73%). ^{1}H NMR (500 MHz, D_2O): δ (ppm) = 7.96 (s, 3H, -C=C*H*-), 7.42–7.36 (m, 5H, aryl H), 5.03 (s, 2H, benzyl H), 4.57 (brt, 6H, -NHC*H*$_2$$CH_2$-), 4.02–3.49 (m, 99H, SA (8-H, NH, 7-H, 4-H, 9-H, 5-H, 6-H,) -SC*H*$_2$C=C-, EG spacer), 3.33 (br t, 6H, -CH_2C*H*$_2$$N_3$-), 2.78 (d, ^3J = 10 Hz, 3H, SA 3-He), 2.19 (br t, 6H,—CH_2C*H*$_2$CONH-), 2.00 (s, 9H, SA -NHCOC*H*$_3$), 1.88 (m, 6H, -C*H*$_2$$CH_2$CONH-), 1.75 (t, 3H, ^3J = 10 Hz, SA 3-Ha); ^{13}C NMR (125 MHz, D_2O): δ (ppm) = 175.9, 128.9, 124.9, 74.9, 71.9, 69.7–69.6, 68.9, 68.8,68.7, 68.2, 62.67, 51.8, 50.2, 40.8, 39.2, 38.0 30.0, 23.9, 23.8, 22.1; IR (film): ν = 3350, 2923, 1597, 1446, 1371, 1349, 1113, 1078, 986, 935, 903, 857 cm^{-1}; HRMS (ESI): *m/z*: calcd for $C_{120}H_{170}N_{16}O_{47}S_3$: 2550.9982 [$M+2Na^+ + K^+ - 1$]; found 2550.9737.

Synthesis of the compound cbzTris(propargyl)$_3$ 19

Cbz-protected triacid (950 mg, 2.49 mmol) was dissolved in 15 mL of dry DMF and cooled to 0 °C (ice bath). Then triethylamine (1.56 mL, 11.18 mmol), EDC·HCl (2.14 g, 11.16 mmol) and DMAP (638 mg, 5.22 mmol) were added, and the reaction mixture was stirred at 0 °C for 20 minutes. Then propargyl amine (0.717 mL, 11.19 mmol) was added and stirred for 72 h at room temperature. The solution was diluted with ethyl acetate (70 mL) and washed with 1 M HCl (3×20 mL), water (40 mL), and brine (2×20 mL). The organic phase was dried over Na_2SO_4, and the solvent was removed under reduced pressure. The crude product was purified by column chromatography with a DCM/methanol mixture. (732 mg, 60%). ^{1}H NMR (500 MHz, [D_6]DMSO): δ (ppm) = 8.24 (t, ^3J = 10 Hz, 3H, -N*H*CH_2-), 7.36–7.29 (m, 5H, aryl H), 4.98 (s, 2H, benzyl H), 3.83–3.82 (m, 6H, -C*H*$_2$CCH-), 3.08 (t, ^5J = 5 Hz, 3H, -CH_2CC*H*-), 2.03 (brt, 6H, -CH_2C*H*$_2$CONH-), 1.77 (brt, 6H, -C*H*$_2$$CH_2$CONH-); ^{13}C NMR (125 MHz, $CDCl_3$): δ (ppm) = 173.4, 155.2, 137.3, 128.9, 128.4, 80.0, 71.9, 66.6, 57.5, 31.2, 30.7, 29.5; IR (film): ν = 3289, 3057, 2939, 1704, 1644, 1525, 1242, 1057, 1027, 926, 732 cm^{-1}; HRMS (ESI): *m/z*: calcd for $C_{27}H_{32}N_4O_5$: 515.5658 [$M+Na^+$]; 531.5397 [$M+K^+$]; found: 512.2291, 531.2023 respectively.

Synthesis of the compound cbzTris(EG_1N_3)$_3$ 20

The coupling of cbzTris(propargyl)$_3$ (240 mg, 0.56 mmol) and azido ethyl tosylate (459 mg, 1.90 mmol) using copper assisted click reaction followed by azidation was performed like **22**. (342.28 mg, 75%). ^{1}H NMR (500 MHz, [D_6]DMSO): δ (ppm) = 7.83 (s, 3H, -C=CH-), 7.26–7.18 (m, 5H, aryl H), 4.92 (s, 2H, benzyl H), 4.46 (t, ^3J = 5 Hz, 6H, -C*H*$_2$$CH_2N_3$); 4.34 (s, 6H, -CONHC*H*$_2$-), 3.71 (t, ^3J = 5 Hz, 6H, -CH_2C*H*$_2$$N_3$); 2.14 (t, 6H, ^3J = 5 Hz, -CH_2C*H*$_2$CONH-), 1.87 (t, ^3J = 5 Hz, 6H, -C*H*$_2$$CH_2$CONH-); ^{13}C NMR (125 MHz, CD_3OD): δ (ppm) = 175.6, 156.6, 146.5, 129.4, 128.7, 124.8 66.9, 57.9 51.7, 50.5, 35.6, 31.5, 31.0; IR (film): ν = 3287, 2925, 2107, 1712, 1678, 1529, 1455, 1240, 1061 cm^{-1}; HRMS (ESI): *m/z*: calcd for $C_{33}H_{44}N_{22}O_5$: 851.3763 [$M+Na+$]; found: 851.3788.

Synthesis of the compound cbzTris(EG_1SA)$_3$ 21

The coupling of cbzTris(EG_1N_3)$_3$ **20** (32 mg, 0.04 mmol) and prop-2-ynyl α-thiosialoside (81.9 mg, 0.015 mmol) using copper-assisted click reaction and further deprotection was performed similarly to **18** (49.28 mg, 69%). ^{1}H NMR (500 MHz, D_2O): δ (ppm) = 7.81 (br s, 3H, -C=CH-), 7.58 (br s, 3H, -C=CH-), 7.26–7.22 (m, 5H, aryl H), 4.89 (s, 2H, benzyl H), 4.22–3.43 [m, 42H SA (8-H, 7-H, 4-H, 9-H, 5-H, 6-H,) SC*H*$_2$C=C, -CONHC*H*$_2$-, ethylene spacer], 2.68 (br s, 3H, SA 3-He), 2.13 (br s, 6H, -CH_2C*H*$_2$CONH-), 1.91 (s, 9H, SA -NHCOC*H*$_3$), 1.80 (br s, 7H, -C*H*$_2$$CH_2$CONH-, SA 3-Ha); ^{13}C NMR (125 MHz, D2O): δ (ppm) = 175.7, 174.9, 136.7, 130.2, 129.4, 128.6, 128.1, 127.6, 74.8, 71.3, 68.0, 62.7, 51.6, 49.8, 40.2, 34.5, 29.7, 22.0; IR (film): ν = 3317, 2971, 1647, 1557, 1374, 1364, 1032, 1013 cm^{-1}; HRMS (ESI): *m/z*: calcd for $C_{75}H_{107}N_{25}O_{29}S_3$: 1960.6613 [$M+2Na^+ - 3$]; found: 1960.6398.

Synthesis of the compound cbzTris(EG_4N_3)$_3$ 22

The $TsOEG_4N_3$ was synthesized by reported procedure of Xuyi Yue et al.[12a] The cbzTris(propargyl)$_3$ **19** (200 mg, 0.47 mmol) and $TsOEG_4N_3$ (590 mg, 1.58 mmol) were dissolved in DMF. $CuSO_4$·5H_2O (21 mg, 0.08 mmol) was dissolved in 0.2 mL of H_2O and added to the solution of sodium ascorbate (217 mg, 1.10 mmol) in 0.4 mL H_2O. The resultant solution of salts in water was added drop wise to the solution containing $TsOEG_4N_3$ and cbzTris(popargyl)$_3$. The reaction mixture was degassed with argon for 10 minutes and then allowed to stir at 40 °C for 48 h. The completion of reaction was monitored by TLC. It was followed by in situ azidation with NaN_3 (308 mg, 4.74 mmol), at 70 °C for 24 h. The stirring was stopped, and solvent was removed under reduced pressure. The crude product was purified by column chromatography with a DCM/methanol mixture. (414.2 mg, 72%). ^{1}H NMR (700 MHz, [D_4]MeOH) δ: (ppm) = 7.90 (s, 3H, -C=CH-), 7.34–7.26 (m, 5H, aryl H), 5.00 (s, 2H, benzyl H), 4.54 (t, ^3J = 7 Hz, 6H, -TrzC*H*$_2$$CH_2$O-); 4.41 (s, 6H, -CONHC*H*$_2$-), 3.87 (t, ^3J = 7 Hz, 6H, -TrzCH_2C*H*$_2$O-), 3.64–3.59 (m, 24H, EG spacer), 3.35 (t, 6H, ^3J = 7 Hz, -CH_2C*H*$_2$$N_3$), 2.22 (br t, 6H, -$CH_2$C*H*$_2$CONH-), 1.95 (br t, 6H, -C*H*$_2$$CH_2$CONH-); ^{13}C NMR (125 MHz, [D_6]CD_3OD): δ (ppm) = 175.4, 156.5, 145.9, 138.4, 129.4 128.9, 128.7, 124.9, 171.5–71.0, 70.3, 66.8, 57.8, 51.7, 51.3, 35.7, 31.6, 31.0; IR (film): ν = 3301, 2921, 2868, 2106, 1717, 1650, 1533, 1455, 1244, 1098, 1058,

935 cm^{-1}; HRMS (ESI): *m/z*: calcd for $C_{51}H_{80}N_{22}O_{14}$: 1247.6122 [$M+Na^+$]; found: 1247.6217.

Synthesis of the compound cbzTris(EG_4SA)$_3$ 23

The coupling of cbzTris(EG_4N_3)$_3$ **22** (108 mg, 0.088 mmol) and prop-2-ynyl α-thiosialoside (187 mg, 0.34 mmol) using copper assisted click reaction and further deprotection was performed similarly to **18** (154 mg, 77%). ^{1}H NMR (500 MHz, D_2O): δ (ppm) = 7.90 (s, 3H, -C=CH-), 7.86 (s, 3H, -C=CH-), 7.32–7.29 (m, 5H, aryl H), 4.96 (s, 2H, benzyl H), 4.54 (t, 12H, -Trz$CH_2$$CH_2$O-, -O$CH_2$$CH_2$Trz-), 4.36 (br s, 6H, -NHCH_2Trz-), 4.01–3.48 [m, 63H, SA (8-H, NH, 7-H, 4-H, 9-H, 5-H, 6-H,) SCH_2C=C, EG spacer], 2.75 (dd, ^3J = 14 Hz, ^2J = 7 Hz, 3H, SA 3-He), 2.19 (br t, 6H, -$CH_2$$CH_2$CONH-), 2.01 (s, 9H, SA, -NHCOCH_3), 1.89 (br s, 6H, -$CH_2$$CH_2$CONH-), 1.79 (t, ^3J = 14 Hz, 3H, SA 3-Ha); ^{13}C NMR (125 MHz, D_2O): δ (ppm) = 175.67, 175.17, 172.72, 144.59, 128.86, 128.38, 127.62, 124.9, 124.5, 84.3, 75.0, 71.4, 69.8, 69.6, 68.8, 68.7, 68.2, 62.9, 56.9, 51.8, 40.3, 34.6, 29.9, 23.3, 22.2; IR (film): ν = 3280, 2927, 1705, 1645, 1548, 1114, 1059, 1027, 954 cm^{-1}; HRMS (ESI): *m/z*: calculated for $C_{93}H_{143}N_{25}O_{38}S_3$: 2335.9080 [$M+Na^+-1$]; found: 2335.8764.

Hemagglutination inhibition assay

Inhibitors were twofold serially diluted in PBS. Then, 4 HAU X31 virus containing approximately 4×10^7 virus particles were added to all the wells. The amount of virus particles per volume was estimated as published by Desselberger et al.[20] After 30 min incubation under slight agitation at rt, 50 μL of a 1% human erythrocyte solution (German Red Cross, $\approx2\times10^6$ cells per μL) was added, gently mixed, and incubated for 60 min at rt. The inhibitor constant K_{iHAI}, reflects the lowest inhibitor concentration, which is necessary to achieve full inhibition of virus induced hemagglutination. To check for full hemagglutination inhibition, the microtiter plate was tilted by 60° to cause droplet formation from the red blood cell pellet.[21]

Microscale thermophoresis (MST)

Measurements have been performed using a Monolith NT.115 instrument (Nanotemper) and standard glass capillaries. For safety reasons, X31 was inactivated with UV light for 5 min on ice. Then the envelope of viruses (1 mg mL^{-1} protein) was labeled at 20 μM R18 for 30 min at rt under gentle shaking. Unbound R18 was removed under centrifugation at 20,000 *x* g for 5 min. The resuspended virus was filtered through a 0.45 μm filter (Millipore) to remove virus aggregates. To quantify the amount of virus and to check whether the prepared virus was still able to bind, a hemagglutination assay was performed. Each inhibitor was twofold serially diluted and mixed with equal amounts of X31 (4 HAU). After a short incubation, then the inhibitor-virus mix was loaded on glass capillaries and measured at rt for initial fluorescence (5 s) and change in fluorescence over time (30 s) with the thermophoresis measurement (MST power: 80%, green LED power 100%). The T-jump with thermophoresis was used for analysis. Data were analyzed by with Graph pad Prism 5 using a one-sided fit with a cooperativity factor of 1. In order to determine the noise level, triplicates of the same virus dilution were measured leading to $\Delta F = 5$ FU. For safety reasons X31 was inactivated with UV light for 5 min on ice. The change in fluorescence was expressed as ΔFnorm (‰) and represented values after subtraction of background and correlation to the initial fluorescence before IR laser activation.

Molecular dynamics simulation set-up

All-atom molecular dynamics (MD) simulations were performed for the monovalent counterparts of compounds **8** and **9** (later referred as ligands **8** and **9**, respectively) in explicit water (TIP3P water model),[22] using the GROMACS 5.0.2 simulation package.[23] The initial structures of the ligands were drawn in Marwin Sketch (MarvinSketch (version 6.2.2, calculation module developed by ChemAxon), http://www.chemaxon.com/products/marvin/marvinsketch/, 2014). Both ligands were parametrized in Acpype.[24] The topologies of the ligands **8** and **9** were generated according to the General Amber Force Field (GAFF).[25] The semi-empirical quantum chemistry program SQM[26] was used to assign the partial charges with the AM1-BC level of theory. The systems were minimized in vacuum with the steepest decent algorithm[27] (emtol = 1000.0 (kJ mol^{-1}) nm^{-1}, nsteps = 50 000). 4069 and 14441 water molecules were added to solvate the ligands **8** and **9**, respectively, in a dodecahedron box (volume of the ligand **8** box 130.51 nm^3, volume of the ligand **9** box 443.76 nm^3). Then solvated ligands were brought to another round of minimization with the same parameters, followed by two equilibration runs, first in the NVT ensemble at 300 K (V-rescale thermostat,[28] time constant = 0.1 ps), and then in NPT ensemble (Parrinello–Rahman barostat,[29] reference pressure = 1 bar, time constant = 2 ps) for 100 ps, respectively. Five starting structures per ligand were randomly taken from the NPT equilibration run and later used in the subsequent MD runs. The production runs were simulated in the NPT ensemble (temperature 300 K, pressure 1 bar). The covalent bonds to all hydrogen atoms were constrained with the LINCS algorithm[30] (lincs iter = 1, lincs order = 4), allowing for an integration time step of 2 fs. Newton's equations of motion were integrated with a leap-frog Scheme. The cut-off for Lennard-Jones interactions was set to 1 nm. The electrostatic interactions were treated with the particle-mesh ewald (PME) algorithm[31] with a real space cut off 1 nm, a Fourier grid spacing of 0.16 nm, and an interpolation order of 4. Periodic boundary conditions were applied in all three dimensions. The solute coordinates were written to the trajectory file every 1 ps. In total, 1 μs of the simulations were obtained for each ligand.

Molecular dynamics data analysis

The respective distances used to characterize ligands **8** and **9** were obtained with the GROMACS command g_mindist. Then, they were visualized with an in-house MATLAB[31] script. The intramolecular hydrogen bond networks were computed with GROMACS command g_hond, while the radius of gyration was extracted from the respective trajectories with GROMACS command g_gyrate.

Supporting information

Details on the synthesis of heterobifunctional oligoethylene spacers, sialic acid derivative, and control molecule **24**. Model for trivalent and divalent sialoside binding.

Acknowledgements

This contribution was generously supported by the German Research Foundation (DFG, SFB765) and the EU-Innovative Training Network, Multi-App. We thank Professor Dr. Joachim Heberle for giving us the opportunity to perform MST measurements in his lab. We acknowledge Dr. Pamela Winchester for careful language polishing of the manuscript. The comput-

er facilities of the Freie Universität Berlin (ZEDAT) are acknowledged for the computer time.

Conflict of interest

The authors declare no conflict of interest.

Keywords: adamantane · influenza inhibitors · oligoethylene glycol · trivalent sialoside · viruses

[1] a) E. Vanderlinden, L. Naesens, *Med. Res. Rev.* **2014**, *34*, 301 – 339; b) C. A. Russell, T. C. Jones, I. G. Barr, N. J. Cox, R. J. Garten, V. Gregory, I. D. Gust, A. W. Hampson, A. J. Hay, A. C. Hurt, J. C. de Jong, A. Kelso, A. I. Klimov, T. Kageyama, N. Komadina, A. S. Lapedes, Y. P. Lin, A. Mosterin, M. Obuchi, T. Odagiri, A. D. M. E. Osterhaus, G. F. Rimmelzwaan, M. W. Shaw, E. Skepner, K. Stohr, M. Tashiro, R. A. M. Fouchier, D. J. Smith, *Science* **2008**, *320*, 340 – 346.

[2] a) J. J. Skehel, D. C. Wiley, *Ann. Rev. Biochem.* **2000**, *69*, 531 – 569; b) M. Mammen, S.-K. Choi, G. M. Whitesides, *Angew. Chem. Int. Ed.* **1998**, *37*, 2754 – 2794; *Angew. Chem.* **1998**, *110*, 2908 – 2953; c) A. Bernardi, J. Jiménez-Barbero, A. Casnati, C. De Castro, T. Darbre, F. Fieschi, J. Finne, H. Funken, K.-E. Jaeger, M. Lahmann, T. K. Lindhorst, M. Marradi, P. Messner, A. Molinaro, P. V. Murphy, C. Nativi, S. Oscarson, S. Penadés, F. Peri, R. J. Pieters, O. Renaudet, J.-L. Reymond, B. Richichi, J. Rojo, F. Sansone, C. Schäffer, W. B. Turnbull, T. Velasco-Torrijos, S. Vidal, S. Vincent, T. Wennekes, H. Zuilhof, A. Imberty, *Chem. Soc. rev.* **2013**, *42*, 4709 – 4727; d) W. Weis, J. H. Brown, S. Cusack, J. C. Paulson, J. J. Skehel, D. C. Wiley, *Nature* **1988**, *333*, 426 – 431.

[3] V. Bandlow, S. Liese, D. Lauster, K. Ludwig, R. R. Netz, A. Herrmann, O. Seitz, *J. Am. Chem. Soc.* **2017**, *139*, 16389 – 16397.

[4] S. Bhatia, D. Lauster, M. Bardua, K. Ludwig, S. Angioletti-Uberti, N. Popp, U. Hoffmann, F. Paulus, M. Budt, M. Stadtmüller, T. Wolff, A. Hamann, C. Böttcher, A. Herrmann, R. Haag, *Biomaterials* **2017**, *138*, 22 – 34.

[5] a) M. Waldmann, R. Jirmann, K. Hoelscher, M. Wienke, F. C. Niemeyer, D. Rehders, B. Meyer, *J. Am. Chem. Soc.* **2014**, *136*, 783 – 788; b) M. Yamabe, K. Kaihatsu, Y. Ebara, *Bioconjugate Chem.* **2018**, *29*, 1490 – 1494.

[6] I. A. Wilson, J. J. Skehel, D. C. Wiley, *Nature* **1981**, *289*, 366.

[7] A. Harris, M. J. Borgnia, D. Shi, A. Bartesaghi, H. He, R. Pejchal, Y. Kang, R. Depetris, A. J. Marozsan, R. W. Sanders, P. J. Klasse, J. L. S. Milne, I. A. Wilson, W. C. Olson, J. P. Moore, S. Subramaniam, *Proc. Natl. Acad. Sci. USA* **2011**, *108*, 11440 – 11445.

[8] T. Ohta, N. Miura, N. Fujitani, F. Nakajima, K. Niikura, R. Sadamoto, C. T. Guo, T. Suzuki, Y. Suzuki, K. Monde, S. I. Nishimura, *Angew. Chem. Int. Ed.* **2003**, *42*, 5186 – 5189; *Angew. Chem.* **2003**, *115*, 5344 – 5347.

[9] F. Feng, N. Miura, N. Isoda, Y. Sakoda, M. Okamatsu, H. Kida, S.-I. Nishimura, *Bioorg. Med. Chem. Lett.* **2010**, *20*, 3772 – 3776.

[10] G. D. Glick, P. L. Toogood, D. C. Wiley, J. J. Skehel, J. R. Knowles, *J. Biol. Chem.* **1991**, *266*, 23660 – 23669.

[11] S. Liese, M. Gensler, S. Krysiak, R. Schwarzl, A. Achazi, B. Paulus, T. Hugel, J. P. Rabe, R. R. Netz, *ACS Nano* **2017**, *11*, 702 – 712.

[12] X. Yue, Y. Feng, Y. B. Yu, *J. Fluorine Chem.* **2013**, *152*, 173 – 181.

[13] W. Maison, J. V. Frangioni, N. Pannier, *Org. Lett.* **2004**, *6*, 4567 – 4569.

[14] E. Franzmann, F. Khalil, C. Weidmann, M. Schröder, M. Rohnke, J. Janek, B. M. Smarsly, W. Maison, *Chem. Eur. J.* **2011**, *17*, 8596 – 8603.

[15] D. Claes, M. Holzapfel, N. Clausen, W. Maison, *Eur. J. Org. Chem.* **2013**, 6361 – 6371.

[16] Z. Gan, R. Roy, *Can. J. Chem.* **2002**, *80*, 908 – 916.

[17] H. Ogura, K. Furuhata, M. Itoh, Y. Shitori, *Carbohydr. Res.* **1986**, *158*, 37 – 51.

[18] S. Liese, R. R. Netz, *ACS Nano* **2018**, *12*, 4140 – 4147.

[19] W. J. Lees, A. Spaltenstein, J. E. Kingery-Wood, G. M. Whitesides, *J. Med. Chem.* **1994**, *37*, 3419 – 3433.

[20] U. Desselberger, *Arch. Virol.* **1975**, *49*, 365 – 372.

[21] G. Cross, *Seminars in Avian and Exotic Pet Medicine* **2002**, *11*, 15 – 18.

[22] W. L. Jorgensen, J. Chandrasekhar, J. D. Madura, R. W. Impey, M. L. Klein, *J. Chem. Phys.* **1983**, *79*, 926 – 935.

[23] D. Van Der Spoel, E. Lindahl, B. Hess, G. Groenhof, A. E. Mark, H. J. Berendsen, *J. Comput. Chem.* **2005**, *26*, 1701 – 1718.

[24] A. W. Sousa da Silva, W. F. Vranken, *BMC Res. Notes* **2012**, *5*, 367.

[25] J. Wang, R. M. Wolf, J. W. Caldwell, P. A. Kollman, D. A. Case, *J. Comput. Chem.* **2004**, *25*, 1157 – 1174.

[26] R. C. Walker, M. F. Crowley, D. A. Case, *J. Comput. Chem.* **2008**, *29*, 1019 – 1031.

[27] R. S. Dumont, *J. Comput. Chem.* **1991**, *12*, 391 – 401.

[28] G. Bussi, D. Donadio, M. Parrinello, *J. Chem. Phys.* **2007**, *126*, 014101.

[29] M. Parrinello, A. Rahman, *J. Appl. Phys.* **1981**, *52*, 7182 – 7190.

[30] B. Hess, H. Bekker, H. J. C. Berendsen, J. G. E. M. Fraaije, *J. Comput. Chem.* **1997**, *18*, 1463 – 1472.

[31] T. Darden, D. York, L. Pedersen, *J. Chem. Phys.* **1993**, *98*, 10089 – 10092.

Manuscript received: September 22, 2018
Accepted manuscript online: October 8, 2018
Version of record online: November 22, 2018

